

Supplementary Information

Seed-Directed Synthesis of Chiroptically Active Au Nanocrystals of Varied Symmetries

Jack S. Googasian,^a George R. Lewis,^b Zachary J. Woessner,^a Emilie Ringe,^{b*} and Sara E.

Skrabalak^{a*}

^a Department of Chemistry, Indiana University – Bloomington, 800 E. Kirkwood Ave., Bloomington, IN 47405, USA.

^b Department of Materials Science & Metallurgy, University of Cambridge, 27 Charles Babbage Road, Cambridge, CB3 0FS, UK.

*Corresponding authors: er407@cam.ac.uk, sskrabal@indiana.edu

S.1 Chemicals and Materials:

Gold (III) chloride trihydrate ($\text{HAuCl}_4 \cdot 3\text{H}_2\text{O}$, $\geq 99.9\%$), L-ascorbic acid (L-AA, BioXtra, $\geq 99.0\%$), hexadecyltrimethylammonium bromide (CTAB, BioUltra, $\geq 99.0\%$), cetyltrimethylammonium chloride solution (CTAC, 25 wt. % in H_2O), sodium citrate tribasic dihydrate ($\text{Na}_3\text{Citrate} \cdot 2\text{H}_2\text{O}$, BioUltra, $\geq 99.5\%$), L-Glutathione reduced (L-GSH, $\geq 98\%$), sodium iodide (NaI, 99.999%), and sodium borohydride (NaBH_4 , 99.99%) were purchased from Sigma Aldrich. Sodium hydroxide (NaOH, 99.99%) was purchased from Alfa Aesar. CTAB was recrystallized three times before use; all other chemicals were used as received.

S.2 Nanoparticle Synthesis:

Synthesis of Triangular Au Nanoplates. The synthesis of triangular nanoplates was adapted from a previous literature procedure.¹ To a 20 mL scintillation vial, add 8 mL of water, 1.6 mL of 100 mM CTAC ($\geq 95\%$), and 100 μL of 7.5 mM NaI. Swirl gently for 15 seconds. Add 0.1 mL of 20 mM HAuCl_4 and 8 μL of 100 mM NaOH. Swirl gently for 15 seconds. Add 80 μL of 64 mM L-AA, then swirl for 15 seconds. Add 4 μL of 100 mM NaOH and swirl for 15 seconds. Allow to mature for 25 minutes at room temperature. Solutions will appear blue. The solution was centrifuged (11404 RCF, 10 min) to remove unreacted reagents in the supernatant and the collected pellet was re-dispersed in 1 mL nanopure water for further characterization. Final triangular plate seed solutions were standardized such that a 20:1 dilution of seeds gives an absorbance of 0.246 at 400 nm.

Synthesis of Au Tetrahedra. The synthesis of tetrahedra was adapted from a previous literature procedure and carried out in three steps.²

Step 1: Au Clusters

In a 20 mL vial, prepare 10 mL solution of 100 mM CTAB and 0.025 mM HAuCl₄. Inject 600 μL of 10 mM NaBH₄ and stir rapidly at ~1200 rpm for 2 minutes. Solution will appear brown. Leave undisturbed for 3 hours at room temperature to allow NaBH₄ to decompose.

Step 2: 10 nm Au Spheres

In a 20 mL vial, mix 2 mL of 0.5 mM HAuCl₄, 2 mL of 200 mM CTAC, and 1.5 mL of 100 mM L-AA. Inject 100 μL of the gold clusters from the previous step. Mature solution at room temperature for 10 minutes, then centrifuge at 19,745 RCF for 30 minutes, wash once with water, and redisperse the collected pellet in 1 mL of 20 mM CTAC.

Step 3: Au Tetrahedra

In a 20 mL vial, mix 0.75 mL of water, 0.75 mL of 200 mM CTAC, 0.5 mL of 100 mM CTAB, 1.0 mL of 200 mM L-AA, and 20 μL of 10 nm Au sphere solution in a vial. Stir with a magnetic stir bar while adding 3 mL of 1.0 mM HAuCl₄ from a syringe pump at a rate of 0.5 mL/hr. Allow to mature for 10 minutes after addition finishes, collect via centrifugation at 16363 RCF for 10 minutes, and wash once with water. Final tetrahedral seed solutions were standardized such that a 40:1 dilution of seeds gives an absorbance of 0.186 at 400 nm.

Synthesis of Au Octahedra. The synthesis of octahedra was adapted from a literature procedure.³

In a 30 mL vial, 25 μL of 100 mM HAuCl₄·3H₂O was added to 8.425 mL of water and 1.5 mL of 100 mM CTAB with inversion. 0.050 mL of 100 mM Na₃Citrate was added while the solution was rapidly inverted once. Seeds were matured by suspending the vial in a 110 °C oil bath overnight. Samples were centrifuged (11404 RCF, 10 min) and the collected pellet dispersed into 3 mL of nanopure water. Final octahedral seed solutions were standardized such that a 20:1 dilution of seeds gives an absorbance of 0.252 at 400 nm.

Synthesis of Intrinsically Chiral Au Nanoparticles. The procedure for chiral overgrowth from Au seeds was adapted from previous work.⁴ To a 30 mL vial, add a specified volume of nanopure water, 10 mM HAuCl₄, and a specified amount of surfactant. Gently swirl to mix reagents. Add 475 μ L of 100 mM L-AA followed by a specific volume of 5 mM L-GSH. Next add specific volume of Au nanoplate or tetrahedral seed solution, swirl to ensure proper mixing, and suspend in an oil bath at 30 °C for 2 hr. The product was collected by centrifugation of the reaction solution (11404 RCF, 10 min), with the supernatant being discarded and the collected pellet of nanoparticles being re-dispersed in 1 mL nanopure water for further characterization. The summarized synthesis conditions for each sample are reported below in Table S1.

Table S1. Synthesis conditions for intrinsically chiral nanocrystal samples.

Figure ID	Nanopure Water	10 mM HAuCl ₄	Surfactant	5 mM L-GSH	Seed Volume
1b	3.950 mL	200 μ L	800 μ L of 100 mM CTAB	5 μ L	10 μ L
2b	3.950 mL	200 μ L	320 μ L of 100 mM CTAB 480 μ L of 200 mM CTAC	5 μ L	50 μ L
4a1	3.845 mL	100 μ L	320 μ L of 100 mM CTAB 480 μ L of 200 mM CTAC	5 μ L	50 μ L
4a2	3.745 mL	200 μ L	320 μ L of 100 mM CTAB 480 μ L of 200 mM CTAC	5 μ L	50 μ L
4a3	3.645 mL	300 μ L	320 μ L of 100 mM CTAB 480 μ L of 200 mM CTAC	5 μ L	50 μ L
4a4	3.545 mL	400 μ L	320 μ L of 100 mM CTAB	5 μ L	50 μ L

			480 μ L of 200 mM CTAC		
4b1	3.843 mL	100 μ L	320 μ L of 100 mM CTAB 480 μ L of 200 mM CTAC	7.5 μ L	50 μ L
4b2	3.743 mL	200 μ L	320 μ L of 100 mM CTAB 480 μ L of 200 mM CTAC	7.5 μ L	50 μ L
4b3	3.643 mL	300 μ L	320 μ L of 100 mM CTAB 480 μ L of 200 mM CTAC	7.5 μ L	50 μ L
4b4	3.543 mL	400 μ L	320 μ L of 100 mM CTAB 480 μ L of 200 mM CTAC	7.5 μ L	50 μ L
4c1	3.840 mL	100 μ L	320 μ L of 100 mM CTAB 480 μ L of 200 mM CTAC	10 μ L	50 μ L
4c2	3.740 mL	200 μ L	320 μ L of 100 mM CTAB 480 μ L of 200 mM CTAC	10 μ L	50 μ L
4c3	3.640 mL	300 μ L	320 μ L of 100 mM CTAB 480 μ L of 200 mM CTAC	10 μ L	50 μ L
4c4	3.540 mL	400 μ L	320 μ L of 100 mM CTAB 480 μ L of 200 mM CTAC	10 μ L	50 μ L
S1a	3.950 mL	200 μ L	800 μ L of 100 mM CTAB	0 μ L	10 μ L
S2b	3.950 mL	200 μ L	800 μ L of 100 mM CTAB	5 μ L	50 μ L
S3a	3.950 mL	200 μ L	800 μ L of 100 mM CTAB	5 μ L	50 μ L
S6a	3.950 mL	200 μ L	320 μ L of 100 mM CTAB 480 μ L of 200 mM CTAC	0 μ L	50 μ L

S.3 General Nanoparticle Characterization

CD and extinction measurements were acquired using a Jasco J-715 Circular Dichroism Spectropolarimeter in a quartz cuvette with a path length of 1 cm and sample channel of 1 cm at room temperature. UV-vis-NIR spectra were collected on a Varian Cary 5000 UV-vis-NIR spectrometer at room temperature. Optical characterizations were corrected to water background. Samples for SEM imaging were prepared by drop-casting nanoparticle solutions onto pre-cut Si wafer stubs. After allowing the droplets to dry, the stubs were cleaned by flushing the surface and drawing up small quantities of ethanol several times before imaging. SEM images were obtained with a FEI Quanta FEG 600 Field-Emission Environmental Scanning Electron Microscope or a Zeiss Auriga 60 Focused Ion Beam-Scanning Electron Microscope, both operated at 30 kV with a spot size of 3. For tilt studies, the Zeiss Auriga 60 Focused Ion Beam-Scanning Electron Microscope was operated at 30 kV with a spot size of 3, and images were acquired at 0°, 15°, 30°, and 45°. Selected Area Electron Diffraction (SAED) patterns were acquired on an FEI Tecnai Osiris operating at 200 keV. A double-tilt holder was used to orient each nanoparticle in a 'top-down' orientation, and from this position diffraction patterns were obtained by systematically tilting away, using a small aperture placed around the nanoparticle.

S.4 Tomography Acquisition and Reconstruction Details

TEM samples were prepared by dropcasting 10 μ l of aqueous nanoparticle solutions onto a holey carbon grid. Data was acquired on an FEI Krios operating at 300 keV. For each sample, 100 STEM-HAADF images were acquired, with steps of 1.5° between $\pm 60^\circ$ and steps of 1° from $\pm 60^\circ$ to $\pm 70^\circ$; frames obscured at high angle were removed manually. Image-shift alignment on Sobel-filtered images was then performed using a phase correlation algorithm and tilt-axis

alignment using a manual procedure to minimize arcing in the reconstructions. Tomographic reconstruction was performed using a compressed sensing algorithm formulated as in Goris et al.⁵ with a weighting of 0.05 for the total variation regularization term, implemented with 1000 iterations of a Chambolle-Pock algorithm.⁶ Intensity thresholding and segmentation was then carried out in Avizo to produce the final isosurfaces.

S.5 Finite Difference Time Domain (FDTD) Simulations.

FDTD simulations were performed using Lumerical FDTD Solutions software. The refractive index was set to 1.333. The dielectric functions for the models were fit to optical data collected by Johnson and Christy.⁷ The mesh cells were set to 4 nm to limit simulation time. The left or right circularly polarized (LCP/RCP) source was generated by using two linearly polarized light Total Field Scattered Field sources that are mutually perpendicular along the propagation direction (z-axis), offset by 90° phase difference with a wavelength range of 300 – 1000 nm. STL files were generated from the tomographical reconstructions and imported into the Lumerical software, scaling properly for reconstructed nanocrystal size. Two simulations (one with LCP and one with RCP) were conducted, and the *g*-factor was then calculated from these results. To accurately represent random orientation in solution phase, the reconstruction was rotated in the x- and y-axes from 0-180° in steps of 15°. The final *g*-factor was obtained through averaging across all orientations.

S.6 Supporting Figures

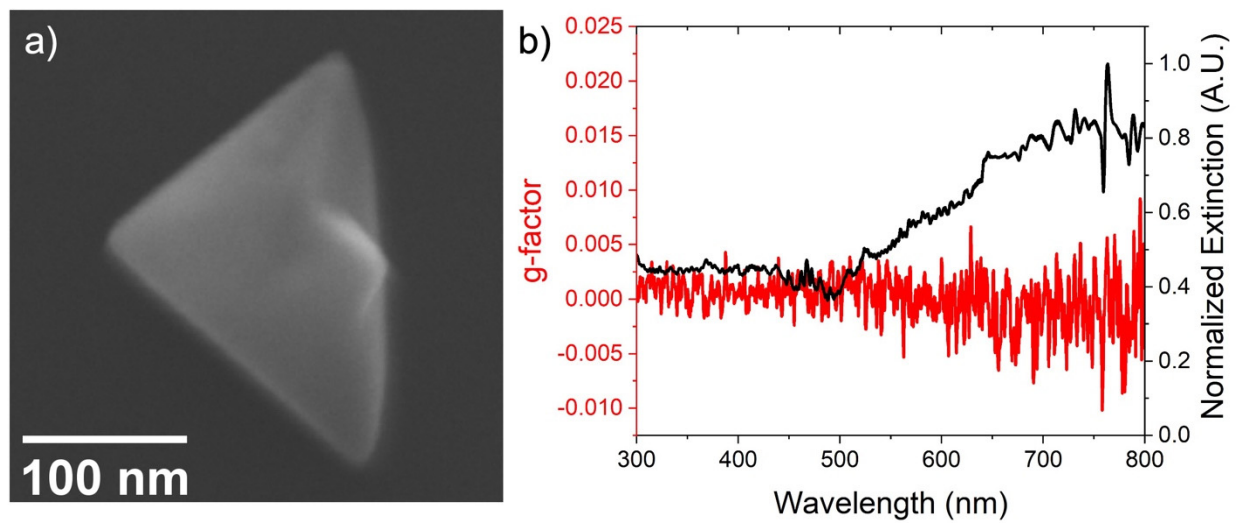


Figure S1. a) SEM image of a characteristic overgrown Au nanoplate product in the absence of L-GSH. b) Normalized extinction and calculated g -factor spectra of the nanocrystal solution.

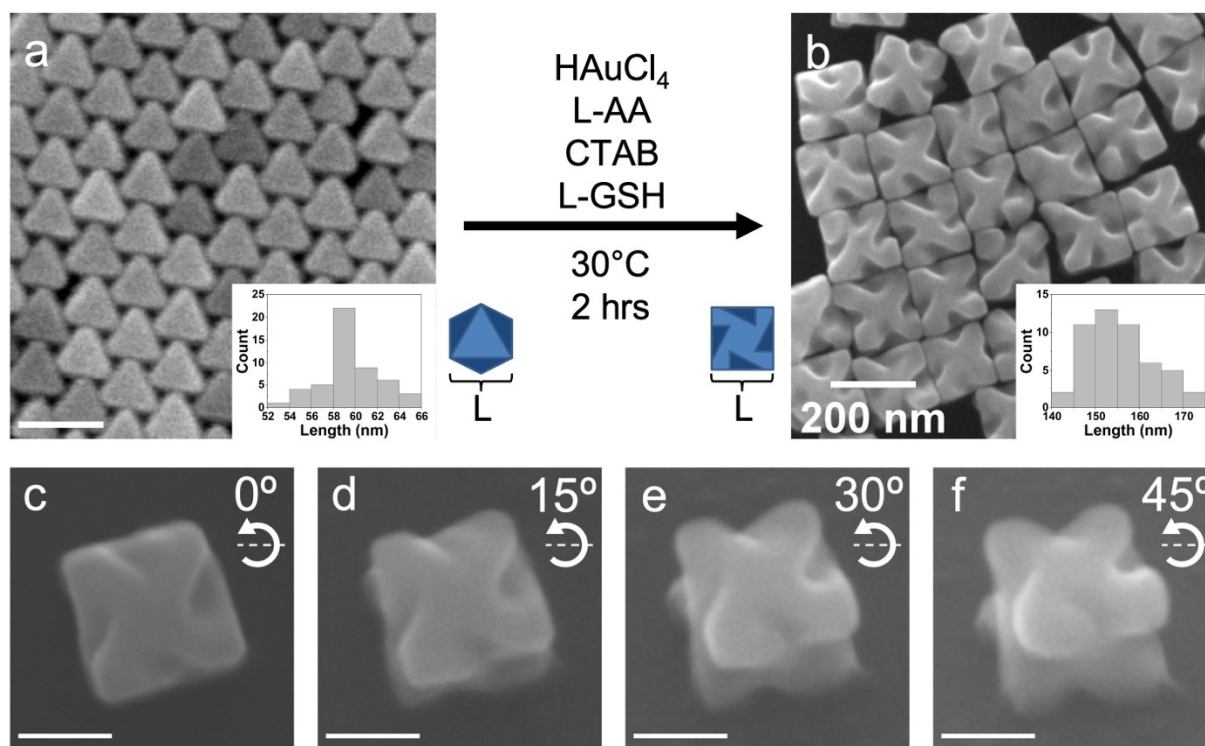


Figure S2. SEM images of a) octahedral Au seeds and b) 432 helicoid III. Insets: histograms of nanocrystal edge lengths. c-f) SEM images of a single 432 helicoid III at tilts denoted in upper right. Scale bars: 100 nm unless otherwise labeled.

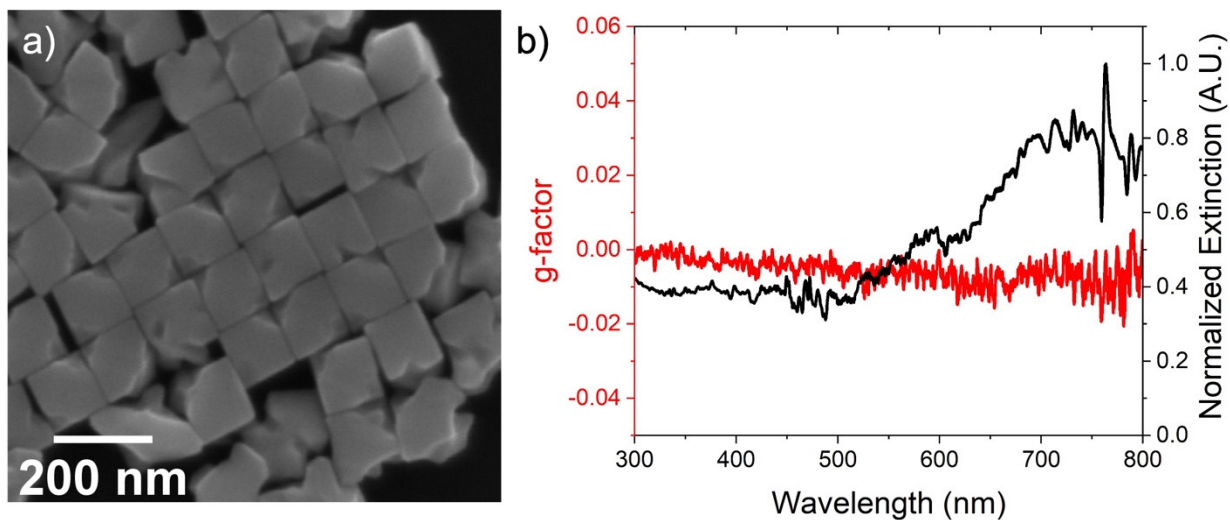


Figure S3. a) SEM image of characteristic overgrown tetrahedral product using only CTAB as the surfactant in the growth solution. b) Normalized extinction and calculated g-factor spectra of the nanocrystal solution.

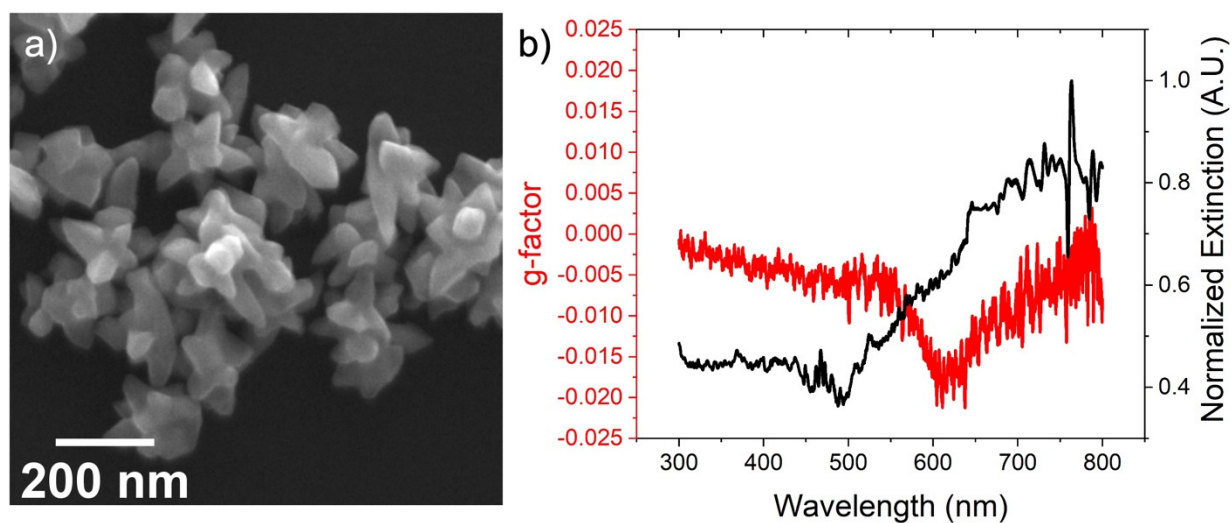


Figure S4. a) SEM image of characteristic overgrowth nanoplate product using the same CTAB/CTAC ratio as in the optimized overgrown tetrahedral seed synthesis. b) Normalized extinction and calculated g -factor spectra of the nanocrystal solution.

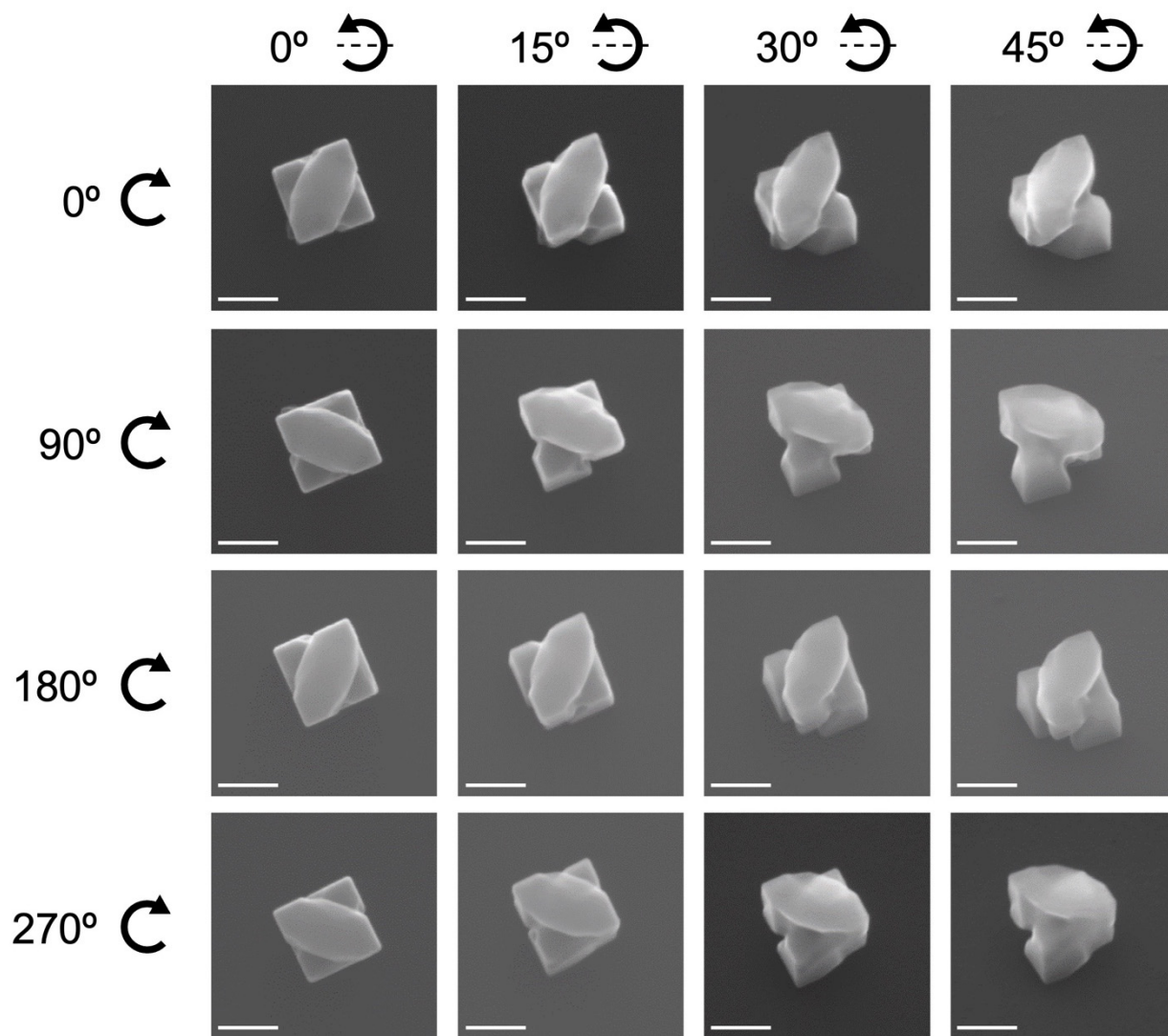


Figure S5. SEM images of overgrowth product from tetrahedral Au seeds. A single nanocrystal is analyzed by tilting the sample from 0 to 45° in 15° increments. Subsequent rows show SEM images of the same nanocrystal rotated in the z-axis to show all sides. Scale bars: 100 nm.

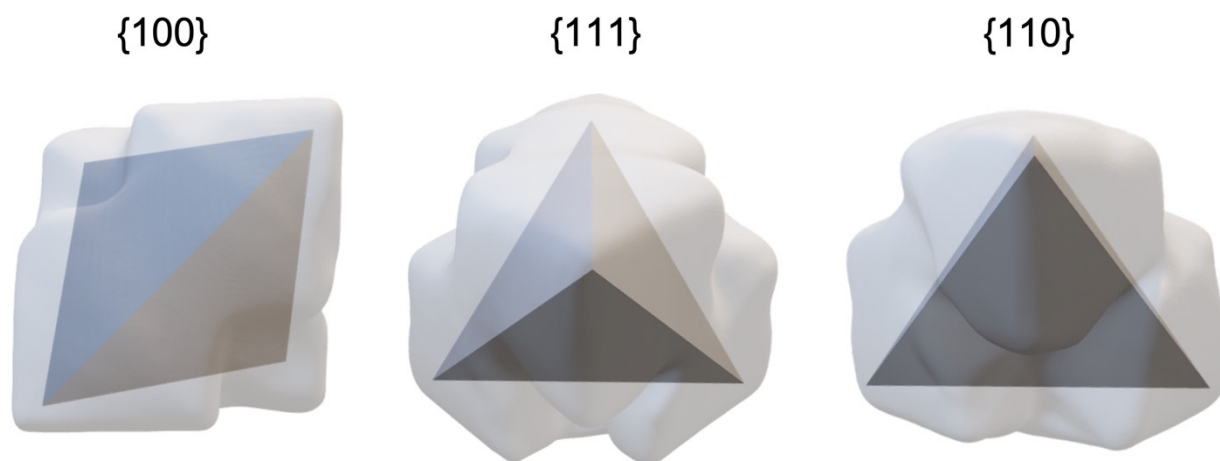


Figure S6. Crystallographic relationship between tetrahedral seed and overgrowth product along the $[100]$, $[111]$, and $[110]$ directions.

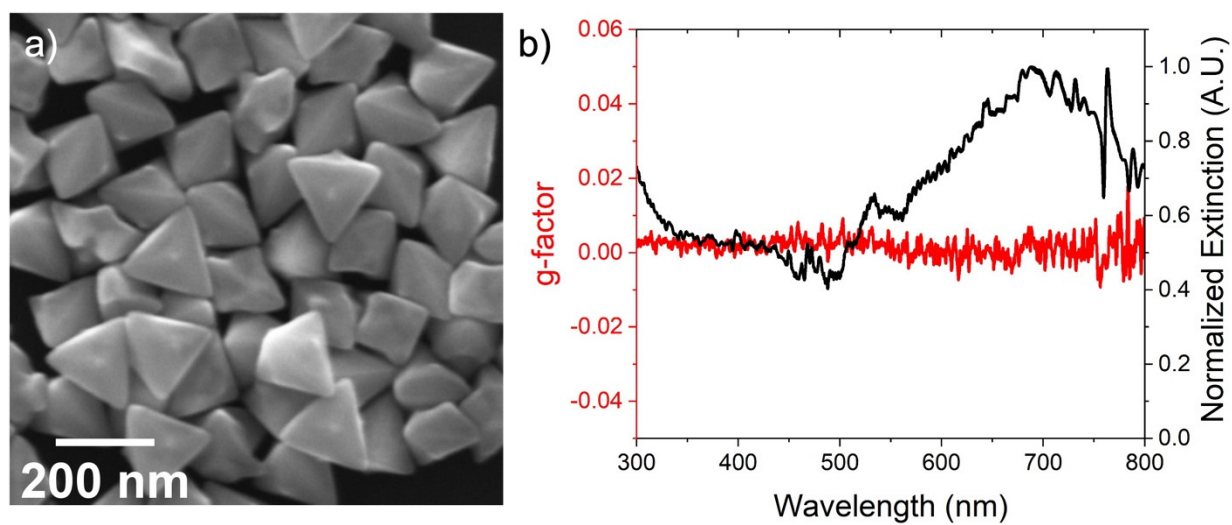


Figure S7. a) SEM image of overgrown tetrahedral product obtained without L-GSH. b) Normalized extinction and calculated g -factor spectra of the nanocrystal solution.

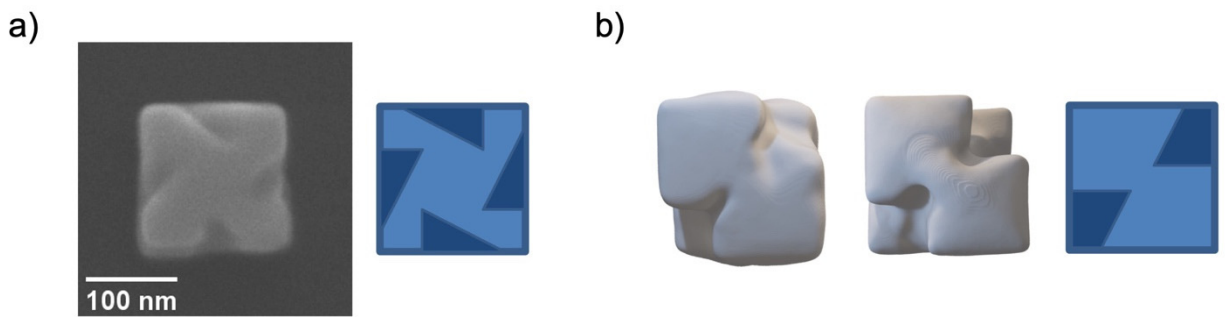


Figure S8. Representative nanocrystal characterizations and cartoon models highlighting clockwise-handed features in a) 432 helicoid III and b) tetrahedral overgrowth product obtained with L-GSH.

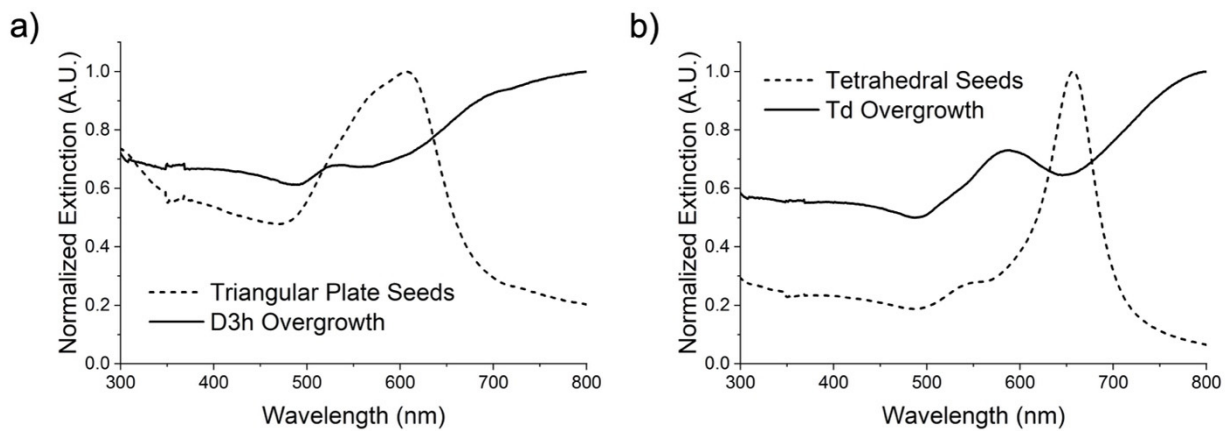


Figure S9. Normalized UV-Visible extinction spectra for a) triangular Au plates and overgrowth product and for b) tetrahedral Au seeds and overgrowth product.

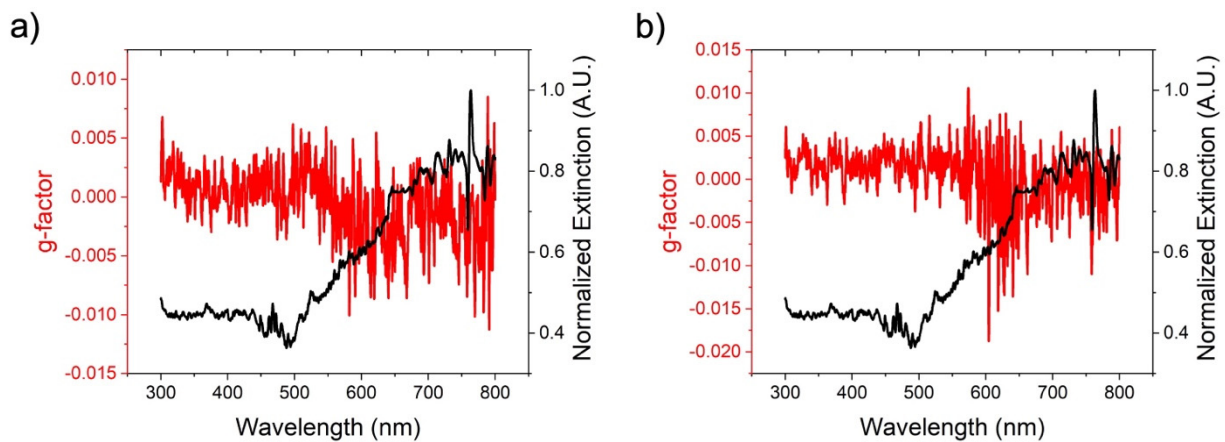


Figure S10. Normalized extinction and calculated g -factor spectra of the a) triangular Au plate seeds and b) tetrahedral seeds.

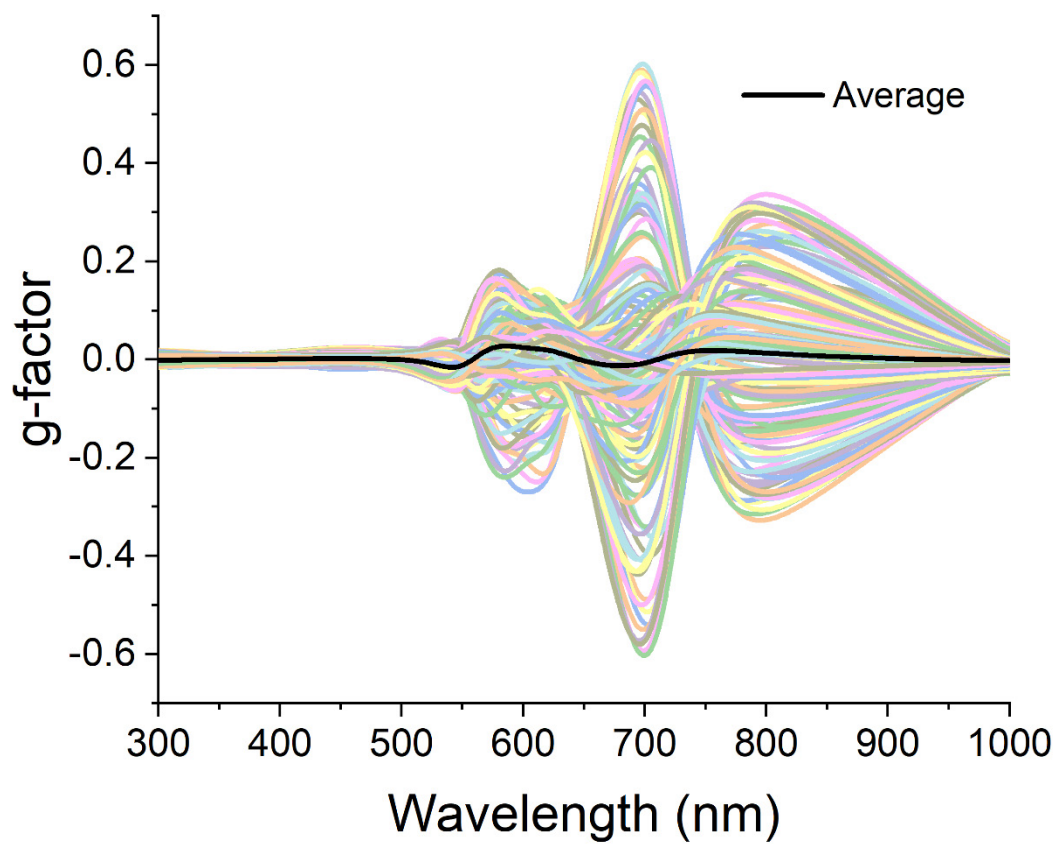


Figure S11. Simulated g -factor spectra for the tomographic reconstruction of an overgrown triangular Au plate over all selected orientations. Average g -factor trace shown in black.

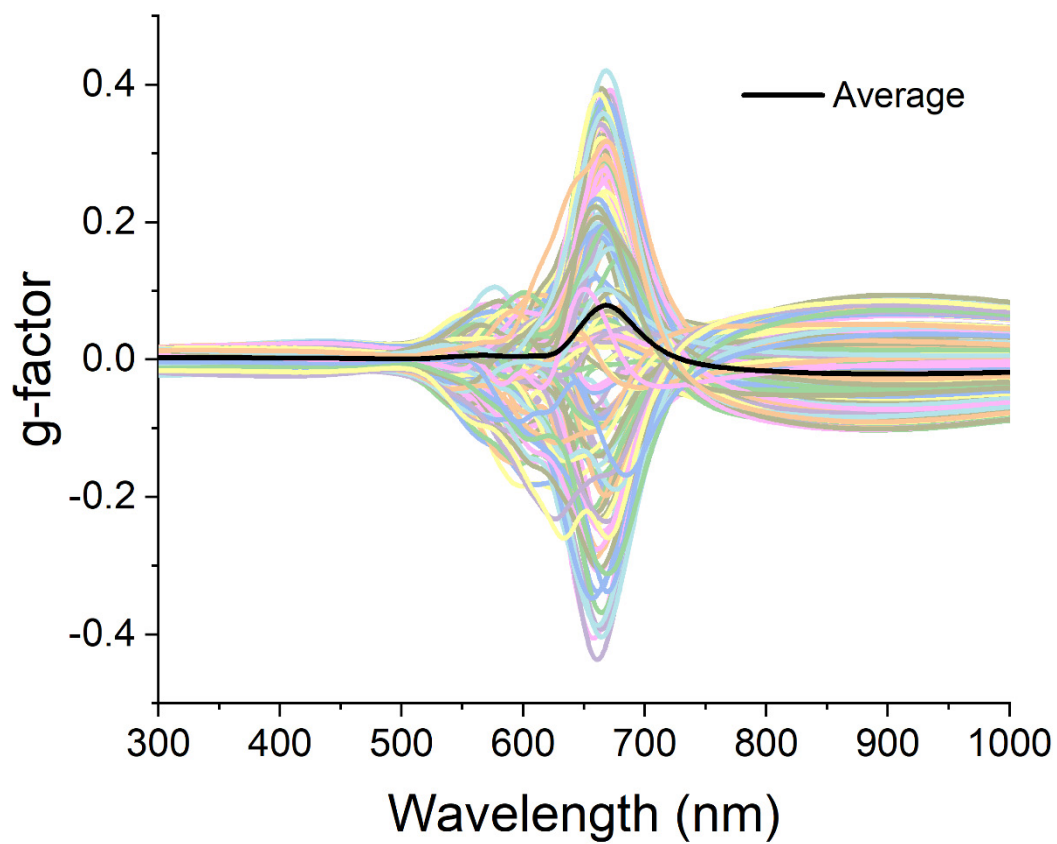


Figure S12. Simulated g-factor spectra for the tomographic reconstruction of an overgrown Au tetrahedron over all selected orientations. Average g-factor trace shown in black.

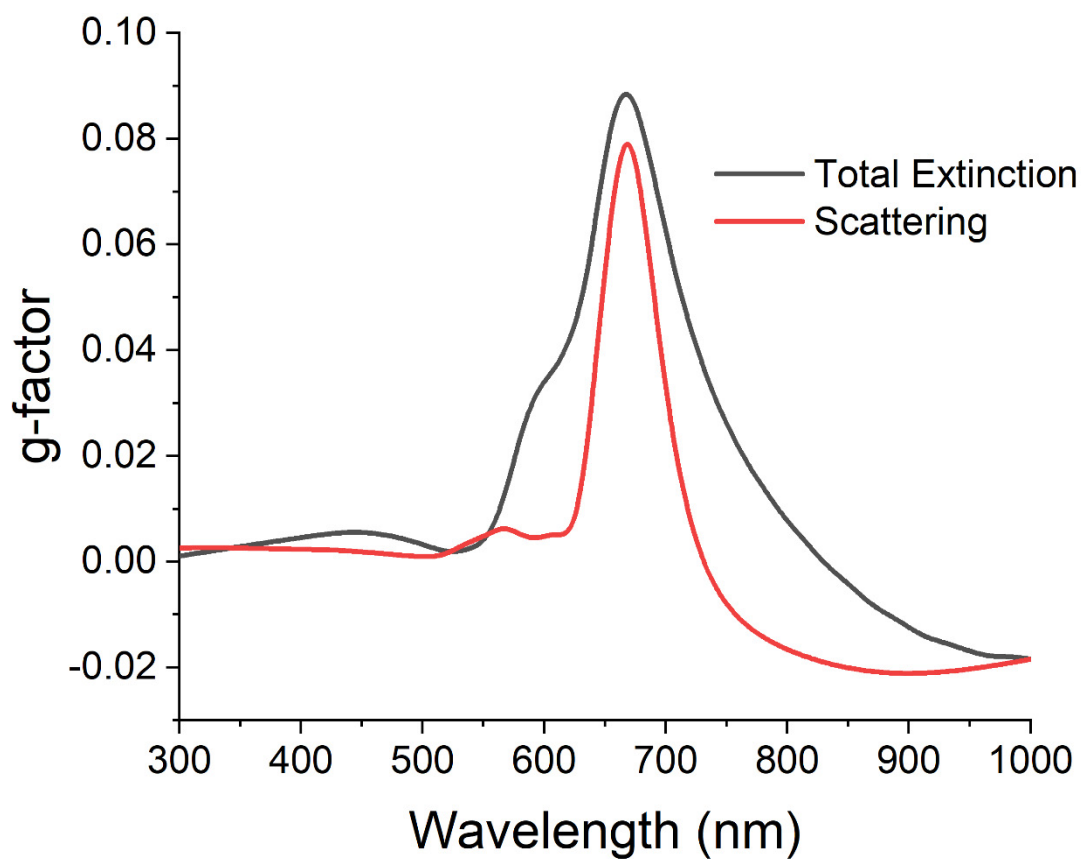


Figure S13. Simulated scattering and total extinction g -factor spectra for the tomographic reconstruction of an overgrown Au tetrahedron averaged over all selected orientations.

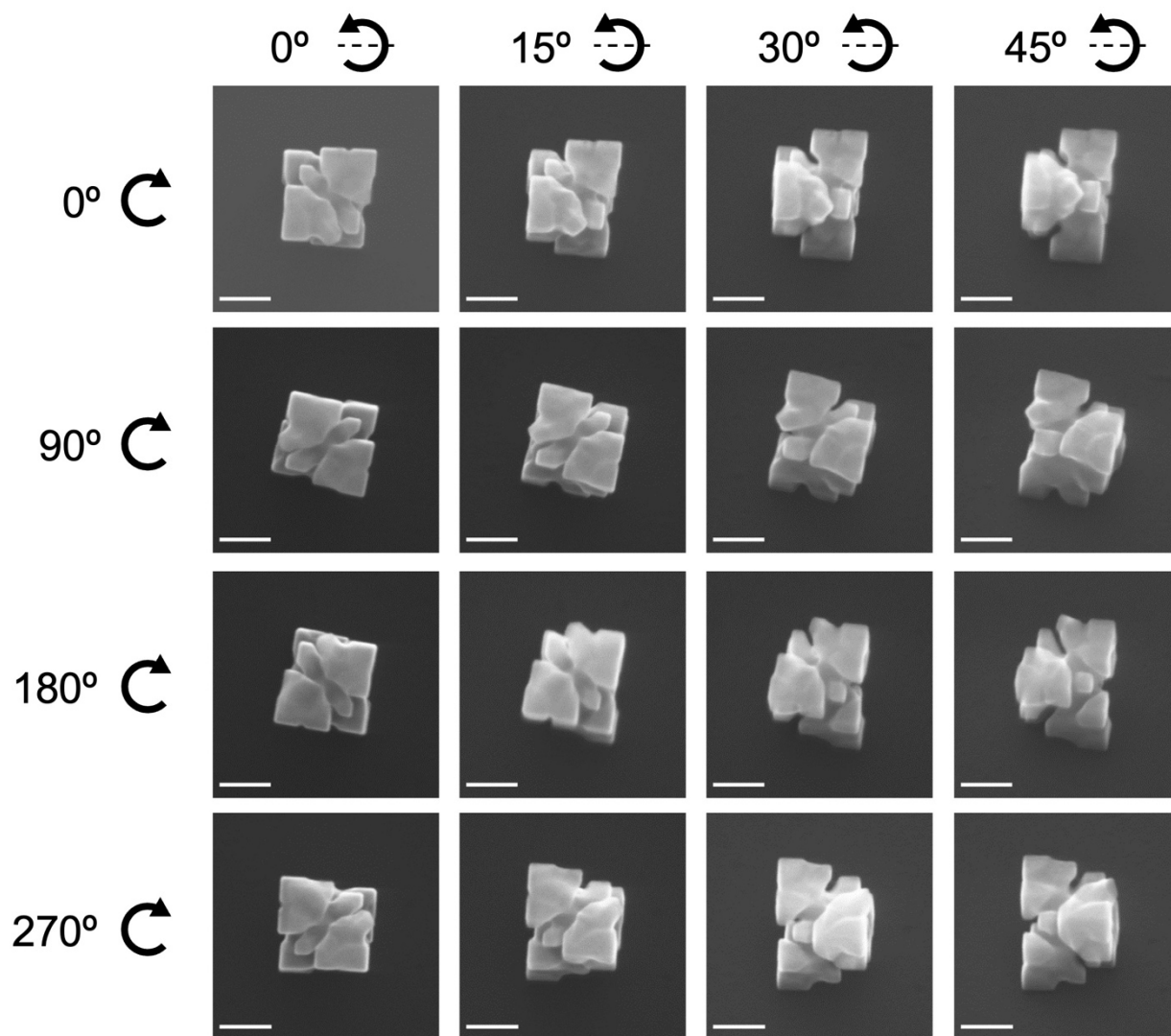


Figure S14. SEM images from a tilt study of a single overgrowth particle from Figure 3, C3, ranging from 0-45°. Subsequent rows show the same particle rotated in the z-axis 90° to show all sides of the particle. Scale bars: 100 nm.

Notes and References

- (1) Kim, J.; Song, X.; Ji, F.; Luo, B.; Ice, N. F.; Liu, Q.; Zhang, Q.; Chen, Q. Polymorphic Assembly from Beveled Gold Triangular Nanoprisms. *Nano Lett.* **2017**, *17* (5), 3270–3275. <https://doi.org/10.1021/acs.nanolett.7b00958>.
- (2) Zheng, Y.; Liu, W.; Lv, T.; Luo, M.; Hu, H.; Lu, P.; Choi, S.-I.; Zhang, C.; Tao, J.; Zhu, Y.; Li, Z.-Y.; Xia, Y. Seed-Mediated Synthesis of Gold Tetrahedra in High Purity and with Tunable, Well-Controlled Sizes. *Chem. – Asian J.* **2014**, *9* (9), 2635–2640. <https://doi.org/10.1002/asia.201402499>.
- (3) Chang, C.-C.; Wu, H.-L.; Kuo, C.-H.; Huang, M. H. Hydrothermal Synthesis of Monodispersed Octahedral Gold Nanocrystals with Five Different Size Ranges and Their Self-Assembled Structures. *Chem. Mater.* **2008**, *20* (24), 7570–7574. <https://doi.org/10.1021/cm8021984>.
- (4) Lee, H.-E.; Ahn, H.-Y.; Mun, J.; Lee, Y. Y.; Kim, M.; Cho, N. H.; Chang, K.; Kim, W. S.; Rho, J.; Nam, K. T. Amino-Acid- and Peptide-Directed Synthesis of Chiral Plasmonic Gold Nanoparticles. *Nature* **2018**, *556* (7701), 360–365. <https://doi.org/10.1038/s41586-018-0034-1>.
- (5) Goris, B.; Van den Broek, W.; Batenburg, K. J.; Heidari Mezerji, H.; Bals, S. Electron Tomography Based on a Total Variation Minimization Reconstruction Technique. *Ultramicroscopy* **2012**, *113*, 120–130. <https://doi.org/10.1016/j.ultramic.2011.11.004>.
- (6) Chambolle, A.; Pock, T. A First-Order Primal-Dual Algorithm for Convex Problems with Applications to Imaging. *J. Math. Imaging Vis.* **2011**, *40* (1), 120–145. <https://doi.org/10.1007/s10851-010-0251-1>.
- (7) Johnson, P. B.; Christy, R. W. Optical Constants of the Noble Metals. *Phys. Rev. B* **1972**, *6* (12), 4370–4379. <https://doi.org/10.1103/PhysRevB.6.4370>.